

# On the *c*-Si surface passivation mechanism by the negative-charge-dielectric Al<sub>2</sub>O<sub>3</sub>

B. Hoex,<sup>a)</sup> J. J. H. Gielis, M. C. M. van de Sanden, and W. M. M. Kessels<sup>b)</sup>

*Department of Applied Physics, Eindhoven University of Technology, P.O. Box 513, 5600 MB Eindhoven, The Netherlands*

(Received 18 June 2008; accepted 29 September 2008; published online 1 December 2008)

Al<sub>2</sub>O<sub>3</sub> is a versatile high- $\kappa$  dielectric that has excellent surface passivation properties on crystalline Si (*c*-Si), which are of vital importance for devices such as light emitting diodes and high-efficiency solar cells. We demonstrate both experimentally and by simulations that the surface passivation can be related to a satisfactory low interface defect density in combination with a strong field-effect passivation induced by a negative fixed charge density  $Q_f$  of up to  $10^{13}$  cm<sup>-2</sup> present in the Al<sub>2</sub>O<sub>3</sub> film at the interface with the underlying Si substrate. The negative polarity of  $Q_f$  in Al<sub>2</sub>O<sub>3</sub> is especially beneficial for the passivation of *p*-type *c*-Si as the bulk minority carriers are shielded from the *c*-Si surface. As the level of field-effect passivation is shown to scale with  $Q_f^2$ , the high  $Q_f$  in Al<sub>2</sub>O<sub>3</sub> tolerates a higher interface defect density on *c*-Si compared to alternative surface passivation schemes. © 2008 American Institute of Physics. [DOI: 10.1063/1.3021091]

## I. INTRODUCTION

An excellent electrical interface quality is essential for many devices relying on the bulk electronic properties of semiconductors.<sup>1</sup> Electrical losses at a semiconductor interface or surface should be minimized in photonic devices based on group III-V or group IV semiconductors when radiative recombination should be the dominant process.<sup>2,3</sup> In complementary metal-oxide-semiconductor (CMOS) devices, the channel is in direct contact with the interface between the gate dielectric and the semiconductor, and therefore interface defect trapping should be minimized.<sup>4</sup> Moreover, electronic losses at the crystalline Si (*c*-Si) surface have become increasingly important in the field of *c*-Si solar cells due to the trend toward thinner *c*-Si wafers used as base material.<sup>5</sup> Consequently, the reduction of recombination losses at semiconductor interfaces is a prime concern for numerous semiconductor applications.

Recombination losses at a semiconductor interface or surface can be reduced by two different passivation strategies. As the recombination rate is directly proportional to the interface defect density, the first strategy is based on the reduction in the number of defect states at the interface. The interface defect density can be reduced significantly by the passivation of undercoordinated atoms (dangling bonds) by, e.g., atomic H or by a thin dielectric or semiconductor film. This strategy is commonly referred to as chemical passivation. For example, the midgap interface defect density of *c*-Si can be as low as  $1 \times 10^9$  eV<sup>-1</sup> cm<sup>-2</sup> after the growth of a high quality thermal SiO<sub>2</sub> film and a subsequent anneal in a H<sub>2</sub> atmosphere, e.g., a forming gas anneal.<sup>6</sup>

The second strategy to reach surface passivation is based on a significant reduction of the electron or hole concentra-

tion at the semiconductor interface by means of a built-in electric field. As recombination processes require both electrons and holes, the highest recombination rate is obtained when the electron and hole concentration at the interface are approximately equal in magnitude (assuming identical capture cross sections for electrons and holes). In other cases the recombination rate scales with the minority carrier concentration at the surface. In the so-called field-effect passivation, the electron or hole concentration at the semiconductor interface is altered by electrostatic shielding of the charge carriers through an internal electric field present at the interface. This internal electric field can either be obtained by a doping profile below the interface or by the presence of fixed electrical charges at the semiconductor interface. Obviously, the principle of field-effect passivation does not apply for CMOS devices such as field effect transistors. A high fixed charge density is even deleterious for the transistor performance as it influences the threshold voltage and the transport of electron and holes in the semiconductor channel.<sup>4,7</sup> Consequently, the application areas of field-effect passivation are limited but the effect can be employed successfully in devices such as light emitting diodes and solar cells.

Recently it was demonstrated that amorphous Al<sub>2</sub>O<sub>3</sub> films synthesized by atomic layer deposition (ALD) yield an excellent level of surface passivation on *c*-Si.<sup>8-13</sup> In our previous work, a similar level of surface passivation as state-of-the-art thermal SiO<sub>2</sub> was demonstrated on low resistivity *n*- and *p*-type *c*-Si,<sup>9</sup> whereas highly doped *p*-type Si surfaces were found to be even more effectively passivated by Al<sub>2</sub>O<sub>3</sub> than by thermal SiO<sub>2</sub>.<sup>10</sup> Remarkably, the Al<sub>2</sub>O<sub>3</sub> films, synthesized by plasma-assisted ALD at a substrate temperature of 200 °C, demonstrated no significant level of surface passivation in the *as-deposited* state.<sup>9,10</sup> A 30 min postdeposition anneal at 425 °C in N<sub>2</sub> was required to obtain the level of surface passivation reported. A nonspecified thermal treatment was also required for an optimal level of surface passivation in the study of Agostinelli *et al.* for Al<sub>2</sub>O<sub>3</sub> films

<sup>a)</sup>Current address: Solar Energy Research Institute Singapore, National University of Singapore, Block E4-01-01, Singapore 117576, Singapore. Electronic mail: bram.hoex@gmail.com.

<sup>b)</sup>Electronic mail: w.m.m.kessels@tue.nl.

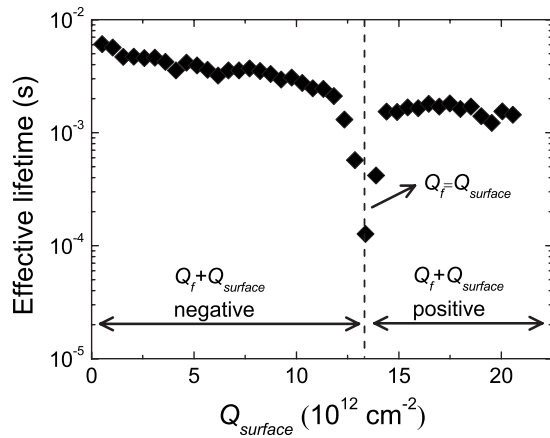


FIG. 1. Effective lifetime of a 1.9  $\Omega$  cm *n*-type *c*-Si wafer passivated on both sides by a 26 nm thick  $\text{Al}_2\text{O}_3$  film. The effective lifetime is presented as a function of the positive charge density  $Q_{\text{surface}}$  deposited at the  $\text{Al}_2\text{O}_3$  on one side of the wafer in a corona charging experiment. Field-effect passivation is ruled by the sum of the negative fixed charge density  $Q_f$  in the  $\text{Al}_2\text{O}_3$  film and the positive  $Q_{\text{surface}}$ . The effective lifetime was determined at an injection level of  $10^{14}$ – $10^{15}$   $\text{cm}^{-3}$ .

synthesized by thermal ALD.<sup>8</sup> The excellent level of surface passivation that can be achieved by ALD-synthesized  $\text{Al}_2\text{O}_3$  films was recently also confirmed at the device level.  $\text{Al}_2\text{O}_3$  applied at the rear of a diffused emitter *p*-type *c*-Si solar cells yielded a conversion efficiency of 20.6%,<sup>12</sup> and  $\text{Al}_2\text{O}_3$  applied at the front side *p*-type emitter of *n*-type solar cells yielded a conversion efficiency of 23.2%.<sup>13</sup>

In this paper, we will address the underlying mechanism of *c*-Si surface passivation as obtained by amorphous  $\text{Al}_2\text{O}_3$  films. From results obtained on  $\text{Al}_2\text{O}_3$  films synthesized by plasma-assisted ALD, it will be demonstrated that in addition to a satisfactory low interface defect density, the surface passivation is ruled for a large part by a strong field-effect passivation induced by a relatively high negative fixed charge density  $Q_f$  in the  $\text{Al}_2\text{O}_3$  film. On the basis of simulations, it will be discussed that the field-effect passivation scales with  $Q_f^2$  and, consequently, the high  $Q_f$  in  $\text{Al}_2\text{O}_3$  tolerates a higher interface defect density than other passivation films with lower  $Q_f$  values. It will be shown that the postdeposition anneal increases the negative  $Q_f$  and lowers the interface defect density of the Si/ $\text{SiO}_x$ / $\text{Al}_2\text{O}_3$  system resulting in a significant improvement of the level of surface passivation obtained. The presence of an interfacial  $\text{SiO}_x$  film between *c*-Si and the  $\text{Al}_2\text{O}_3$  appears to play a key role in both the origin of the negative  $Q_f$  and the interface defect density. As a negative  $Q_f$  in combination with a sufficiently low interface defect density is routinely reported for  $\text{Al}_2\text{O}_3$  films deposited on *c*-Si, irrespective of the deposition technique, it is argued that the findings presented in this paper are not limited to  $\text{Al}_2\text{O}_3$  films synthesized by (plasma-assisted) ALD.

## II. $\text{Al}_2\text{O}_3$ AS NEGATIVE CHARGE DIELECTRIC

The field-effect passivation of *c*-Si by  $\text{Al}_2\text{O}_3$  is experimentally demonstrated in Fig. 1. A high quality 1.9  $\Omega$  cm *n*-type *c*-Si wafer with a thickness of 275  $\mu\text{m}$  was passivated on both sides by a 26 nm thick  $\text{Al}_2\text{O}_3$  film synthesized by plasma-assisted ALD.<sup>11</sup> The resulting effective lifetime of

the passivated *c*-Si wafer exceeds 6 ms indicating that the *c*-Si surfaces are adequately passivated by  $\text{Al}_2\text{O}_3$ . Subsequently a positive charge density  $Q_{\text{surface}}$  is applied at the  $\text{Al}_2\text{O}_3$  surface in a corona charging experiment. In this case, the field-effect passivation is ruled by the sum of  $Q_f$  and  $Q_{\text{surface}}$ . From the figure, it is clear that a positive  $Q_{\text{surface}}$  up to  $10^{13}$   $\text{cm}^{-2}$  hardly affects the effective lifetime of the *c*-Si wafer. However, a positive  $Q_{\text{surface}}$  in the range of  $(1.2\text{--}1.4) \times 10^{13}$   $\text{cm}^{-2}$  leads to a strong decrease in the effective lifetime. A minimum effective lifetime of  $\sim 100$   $\mu\text{s}$  is obtained for a positive  $Q_{\text{surface}}$  of  $1.3 \times 10^{13}$   $\text{cm}^{-2}$ . At this stage, the positive  $Q_{\text{surface}}$  balances the negative  $Q_f$  in the  $\text{Al}_2\text{O}_3$  film, which nullifies the level of field-effect passivation.<sup>11</sup> For a positive  $Q_{\text{surface}}$  exceeding the amount of negative  $Q_f$  [ $Q_{\text{surface}}$  in the range of  $(1.3\text{--}2.0) \times 10^{13}$   $\text{cm}^{-2}$ ] field-effect passivation is provided by the positive charge density at the *c*-Si surface. Summarizing, Fig. 1 clearly demonstrates the mechanism of field-effect passivation on *c*-Si, and it reveals that the negative  $Q_f$  in this 26 nm thick  $\text{Al}_2\text{O}_3$  film is  $(1.3 \pm 0.1) \times 10^{13}$   $\text{cm}^{-2}$ .

$\text{Al}_2\text{O}_3$  has extensively been investigated for the application as gate and charge trapping dielectric on *c*-Si where also high negative  $Q_f$  values have been reported. For gate dielectric applications in CMOS, a low interface defect density and a low  $Q_f$  are essential,<sup>4</sup> whereas a low interface defect density in combination with a high density of electronically active bulk defects is desired for charge trapping dielectrics such as applied in nonvolatile memory.<sup>14,15</sup> Table I summarizes the bulk and interface electronic properties reported in the literature for  $\text{Al}_2\text{O}_3$  films deposited on *c*-Si by various techniques. The sign of  $Q_f$  is always negative for the  $\text{Al}_2\text{O}_3$  films after annealing, irrespective of the deposition technique.<sup>16</sup> The magnitude of  $Q_f$  is typically in the range of  $10^{12}$ – $10^{13}$   $\text{cm}^{-2}$  for annealed  $\text{Al}_2\text{O}_3$  films, in good agreement with our results in Fig. 1. From thickness dependent capacitance-voltage measurements, it was deduced that the negative  $Q_f$  is independent of the  $\text{Al}_2\text{O}_3$  thickness and is located at the interface with the substrate.<sup>17–19</sup>

It is interesting to note that negative fixed charges are detected in  $\text{Al}_2\text{O}_3$  films deposited on H-terminated *c*-Si as well as  $\text{Al}_2\text{O}_3$  films deposited on *c*-Si covered by a 1–100 nm thick  $\text{SiO}_2$  film. Despite the fact that  $\text{Al}_2\text{O}_3$  is thermodynamically stable on *c*-Si,  $\text{Al}_2\text{O}_3$  deposition processes occur under nonequilibrium conditions, and as a result an interfacial  $\text{SiO}_x$  layer is commonly formed between the  $\text{Al}_2\text{O}_3$  film and the *c*-Si substrate.<sup>20–23</sup> This  $\text{SiO}_x$  layer can be formed during the  $\text{Al}_2\text{O}_3$  deposition process but also during the postdeposition annealing treatment. The unintentional formation of an interfacial  $\text{SiO}_x$  is undesired for the application of  $\text{Al}_2\text{O}_3$  as gate dielectric in CMOS devices as it lowers the effective dielectric constant of the layer stack. Nevertheless, only a very limited number of studies (e.g., in the work of Gusev *et al.*<sup>24</sup>) report on the absence of an interfacial  $\text{SiO}_x$  layer between the  $\text{Al}_2\text{O}_3$  film and *c*-Si substrate.<sup>4</sup> An interfacial  $\text{SiO}_x$  film was also detected by high resolution transmission electron microscopy (HR-TEM) in the  $\text{Al}_2\text{O}_3$  films synthesized by plasma-assisted ALD, both in the as-deposited and annealed state, that demonstrated an excellent level of surface passivation on *c*-Si.<sup>9</sup>

TABLE I. Bulk and interface electronic properties for Al<sub>2</sub>O<sub>3</sub> films deposited on *c*-Si as reported in the literature. All films were deposited on H-terminated *c*-Si unless indicated otherwise. In all cases,  $Q_f$  was extracted from the flatband voltage shift determined from capacitance-voltage (*CV*) measurements of MOS structures. The interface defect density was extracted from *CV* and/or conductance measurements of MOS structures. Most samples were analyzed after a postdeposition anneal, however, some samples were also measured as-deposited (indicated with “a-d”).

Negative $Q_f$ (10 <sup>12</sup> cm <sup>-2</sup> )	$D_{it}$ at midgap (10 <sup>11</sup> eV <sup>-1</sup> cm <sup>-2</sup> )	Deposition method	Deposition temperature (°C)	Postdeposition thermal treatment	Ref.
0.2–0.5	...	Pyrolysis of Al(C <sub>3</sub> H <sub>8</sub> O) <sub>3</sub> on <i>c</i> -Si with 23–100 nm thermal SiO <sub>2</sub>	425	30 min FGA <sup>a</sup> at 425 °C	17
0.2–0.5	...	CVD from AlBr <sub>3</sub> +NO on <i>c</i> -Si with 23–100 nm thermal SiO <sub>2</sub>	910	30 min FGA <sup>a</sup> at 425 °C	17
-0.5 (a-d)	15 (a-d)	Pyrolysis of Al(C <sub>3</sub> H <sub>8</sub> O) <sub>3</sub> on <i>c</i> -Si with 1.5 nm native SiO <sub>2</sub>	360	15 min FGA <sup>a</sup> at 510 °C	39
10–11 (a-d)	...	Pyrolysis of AlCl <sub>3</sub> in CO <sub>2</sub> /H <sub>2</sub> environment <sup>b</sup>	900	None	15
0.6 (a-d)	~1	ALD from Al(CH <sub>3</sub> ) <sub>3</sub> +H <sub>2</sub> O	450	None	48
~2	0.8	ALD from Al(CH <sub>3</sub> ) <sub>3</sub> and H <sub>2</sub> O	350	Various at 585 °C and 800 °C	49
...	0.3	Oxidation of evaporated Al	<400	800 °C in N <sub>2</sub>	50
7	1–3	ALD from AlCl <sub>3</sub> and H <sub>2</sub> O <sup>c</sup>	370	None	19
7 (a-d)	13 (a-d)			FGA <sup>a</sup> at 300–450 °C and anneal in N <sub>2</sub> at 450 °C	
6–7	1	ALD from Al(CH <sub>3</sub> ) <sub>3</sub> and H <sub>2</sub> O <sup>b</sup>	350		46
5–10 (a-d)	2–5 <sup>d</sup> (a-d)	Reactive target sputtering in Ar/O <sub>2</sub>	380	FGA <sup>a</sup>	51
...	2–10 (a-d)	ALD from AlCl <sub>3</sub> and H <sub>2</sub> O	300–800	None	52
...	20	ALD from Al(CH <sub>3</sub> ) <sub>3</sub> and H <sub>2</sub> O	300	30 min FGA <sup>a</sup> at 400 °C	53
13 <sup>e</sup> (a-d)	...				
6 <sup>c</sup>	...	ALD from Al(CH <sub>3</sub> ) <sub>3</sub> and O <sub>3</sub>	400	None or 10 min at 800 °C in N <sub>2</sub>	54
		Molecular beam epitaxy from Al and N <sub>2</sub> O on <i>c</i> -Si with an interfacial layer formed from Al and chemical SiO <sub>2</sub> <sup>f</sup>		None or anneal at 600 °C in O <sub>2</sub> , N <sub>2</sub> , H <sub>2</sub> or air	
3–9	...		750		55
3–8 (a-d)	...	ALD from Al(CH <sub>3</sub> ) <sub>3</sub> and H <sub>2</sub> O on <i>c</i> -Si with 7 nm thermal SiO <sub>2</sub>	160–350	None	56
Up to 10	...	ALD from Al(CH <sub>3</sub> ) <sub>3</sub> and H <sub>2</sub> O <sup>b</sup>	<300	Yes, not specified	8
7	...	Remote plasma enhanced CVD from metal organic <sup>g</sup> and O <sub>2</sub> on <i>c</i> -Si <sup>h</sup>	300	30 s anneal at 800 °C and 30 min FGA <sup>a</sup> at 425 °C	18
0.2–2 (a-d)	...				
5–8	...	ALD from Al(CH <sub>3</sub> ) <sub>3</sub> and O <sub>2</sub> plasma	200	30 min anneal at 425 °C	44

<sup>a</sup>Forming gas anneal, typically 5%–10% H<sub>2</sub> in N<sub>2</sub>.

<sup>b</sup>The pretreatment of the *c*-Si wafer was not specified.

<sup>c</sup>The defect density could be lowered by the addition of Zr or Si in the Al<sub>2</sub>O<sub>3</sub> to values in the mid 10<sup>10</sup> eV<sup>-1</sup> cm<sup>-2</sup> range.

<sup>d</sup>The Al<sub>2</sub>O<sub>3</sub> films were grown under UV radiation.

<sup>e</sup>The Al<sub>2</sub>O<sub>3</sub> film was covered with a HfO<sub>2</sub> film.

<sup>f</sup>Polycrystalline Al<sub>2</sub>O<sub>3</sub> was grown in this study due to epitaxy process.

<sup>g</sup>(CH<sub>2</sub>)<sub>3</sub>Al<sub>2</sub>(C<sub>4</sub>H<sub>9</sub>O)<sub>3</sub>

<sup>h</sup>Films were grown at H-terminated *c*-Si and *c*-Si with 1.0 or 1.6 nm thermal SiO<sub>2</sub> with no significant impact on the amount of negative  $Q_f$ .

The origin of the negative  $Q_f$  in Al<sub>2</sub>O<sub>3</sub> deposited on *c*-Si has been attributed to intrinsic and extrinsic defects in Al<sub>2</sub>O<sub>3</sub>. Matsunaga *et al.* calculated the energetics of intrinsic vacancies and interstitials in Al<sub>2</sub>O<sub>3</sub> from first principles.<sup>25</sup> These calculations showed that each intrinsic point defect is most stable in their fully ionized form. Hence, Al vacancies and O interstitials exhibit a negative charge and Al interstitials and O vacancies exhibit a positive charge in good agreement with the ionic nature of the Al<sub>2</sub>O<sub>3</sub>.<sup>25</sup> Extrinsic H has also been proposed as origin for the negative fixed charges in Al<sub>2</sub>O<sub>3</sub>. Peacock and Robertson calculated that interstitial H acts as a deep trap site for electrons in Al<sub>2</sub>O<sub>3</sub>.<sup>26</sup> H is, for example, a common constituent in Al<sub>2</sub>O<sub>3</sub> synthesized by ALD because H-containing precursors such as Al(CH<sub>3</sub>)<sub>3</sub> and H<sub>2</sub>O are used in the deposition process. Hence, Al vacancies, O interstitials, and interstitial H are proposed as the origin of the negative  $Q_f$  in Al<sub>2</sub>O<sub>3</sub>. Based on the ionic nature of Al<sub>2</sub>O<sub>3</sub>, Lucovsky postulated that Al<sub>2</sub>O<sub>3</sub> consists of tetrahedrally coordinated Al in AlO<sub>4</sub><sup>-</sup> units and octahedrally coordi-

nated Al<sup>3+</sup> in a ratio of 3:1 to assure charge neutrality.<sup>27</sup> Kimoto *et al.* demonstrated that both tetrahedrally and octahedrally coordinated Al are present in Al<sub>2</sub>O<sub>3</sub> grown by thermal ALD on H-terminated *c*-Si.<sup>28</sup> However, tetrahedrally coordinated Al was found to be dominant at the interface. This dominance was attributed to the fact that Si in the interfacial SiO<sub>x</sub> film also has a tetrahedral coordination.<sup>28</sup> Consequently, the interfacial SiO<sub>x</sub> film could fulfill an important role in the origin of the negative  $Q_f$  that is found in Al<sub>2</sub>O<sub>3</sub> films grown on *c*-Si by inducing a high density of negatively charged Al vacancies close to the interface. This hypothesis is in good agreement with the location of the negative  $Q_f$  extracted from thickness dependent *CV* measurements by various authors.<sup>17–19</sup>

The polarity of  $Q_f$  plays an important role in the surface passivation of *c*-Si. The most commonly used dielectric passivation films on *c*-Si, i.e., thermal SiO<sub>2</sub>, *a*-SiC<sub>x</sub>:H, and *a*-SiN<sub>x</sub>:H contain a positive  $Q_f$  and lead to a high level of surface passivation of lightly doped *n*- and *p*-type *c*-Si and

highly doped  $n$ -type  $c$ -Si surfaces.<sup>29–31</sup> A positive  $Q_f$  has, however, been shown to be detrimental for the passivation of highly  $p$ -type surfaces such as in  $p$ -type emitters on  $n$ -type solar cells because the minority electrons are attracted to the  $c$ -Si surface and thereby enhance the recombination rate.<sup>10</sup> Positive-charge dielectrics also demonstrate a strong injection level dependence for the surface passivation properties on lightly doped  $p$ -type  $c$ -Si.<sup>31–33</sup> The level of surface passivation decreases when going to lower excess carrier concentrations (i.e., lower injection levels), which is, for example, detrimental for the  $c$ -Si solar cell efficiency under low illumination conditions.<sup>29</sup> This injection level dependence is attributed to additional bulk recombination losses in the inversion layer close to the  $c$ -Si surface.<sup>34</sup> The inversion layer is created by the shielding of holes, which are the majority carriers in the  $p$ -type  $c$ -Si bulk, from the  $c$ -Si surface by the positive  $Q_f$  in the dielectric film. For the negative-charge dielectric  $\text{Al}_2\text{O}_3$  on the other hand, it has been demonstrated that the level of surface passivation is constant at low injection level for lightly doped  $p$ -type  $c$ -Si.<sup>9</sup> On the contrary, when the negative-charge dielectric  $\text{Al}_2\text{O}_3$  is used to passivate lightly doped  $n$ -type  $c$ -Si, the level of surface passivation decreases when going to lower injection level,<sup>9</sup> whereas positive-charge dielectrics demonstrate a constant level of surface passivation in this case.<sup>32,33</sup> Hence, a similar bulk recombination in the inversion layer could explain this injection level behavior of lightly doped  $n$ -type  $c$ -Si passivated by the negative-charge dielectric  $\text{Al}_2\text{O}_3$ . Furthermore, the high positive  $Q_f$  in  $a$ - $\text{SiN}_x$ :H causes the so-called parasitic shunting effect when applied at the rear of  $p$ -type  $c$ -Si solar cells and thereby significantly decreases the short-circuit current of  $c$ -Si solar cells.<sup>35</sup> This effect is absent when the negative-charge dielectric  $\text{Al}_2\text{O}_3$  is used at the rear of diffused front side emitter  $p$ -type  $c$ -Si solar cells, which has resulted in solar cell efficiencies of 20.6%.<sup>12</sup> The negative charge in  $\text{Al}_2\text{O}_3$  is even more important in the passivation of highly doped  $p$ -type  $c$ -Si surfaces as the shielding of the minority carriers, the electrons, from the surface by the negative charges leads to a much higher level of passivation than positive-charge dielectrics such as thermal  $\text{SiO}_2$  and as-deposited  $a$ - $\text{SiN}_x$ :H.<sup>10</sup> The latter was recently also demonstrated at the device level by an exceptionally high conversion efficiency of 23.2% obtained for an  $n$ -type solar cell with a front side B-doped  $p$ -type emitter passivated by a 30 nm thick  $\text{Al}_2\text{O}_3$  film.<sup>13</sup>

### III. FIELD EFFECT PASSIVATION VERSUS CHEMICAL PASSIVATION

It is evident that besides the polarity of the fixed charge, the amount of fixed charge is also important for field-effect passivation. Figure 2 shows the effective surface recombination velocity  $S_{\text{eff}}$  at an injection level of  $5 \times 10^{14} \text{ cm}^{-3}$  (corresponding to approximately 1 sun illumination) as a function of the negative  $Q_f$  located at the surface for moderately doped  $n$ -type ( $[P]=7 \times 10^{15} \text{ cm}^{-3}$ ) and  $p$ -type ( $[B]=7 \times 10^{15} \text{ cm}^{-3}$ )  $c$ -Si. The simulations were performed using the extended Shockley–Read–Hall model as proposed by Girisch *et al.*<sup>36</sup> The fundamental recombination velocities of

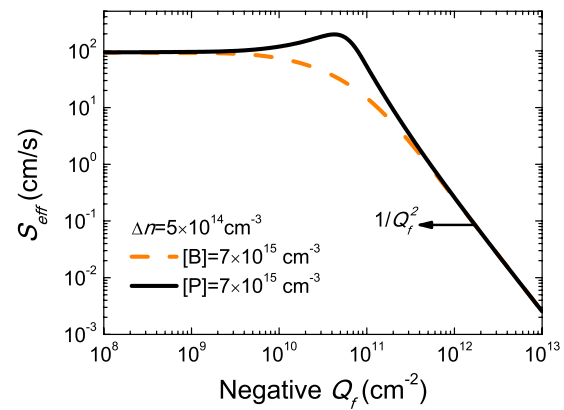


FIG. 2. (Color online) Simulated effective surface recombination velocity  $S_{\text{eff}}$  at an injection level  $\Delta n$  of  $5 \times 10^{14} \text{ cm}^{-3}$  for moderately doped  $n$ -type ( $[P]=7 \times 10^{15} \text{ cm}^{-3}$ ) and  $p$ -type ( $[B]=7 \times 10^{15} \text{ cm}^{-3}$ )  $c$ -Si as a function of the negative  $Q_f$  located at the  $c$ -Si surface.

the electrons and holes were taken to be energy independent and equal to 100 cm/s. Figure 2 clearly shows that a negative  $Q_f$  decreases the  $S_{\text{eff}}$  at a  $p$ -type  $c$ -Si surface. On the other hand, Fig. 2 demonstrates that a relatively small negative  $Q_f$  up to  $5 \times 10^{10} \text{ cm}^{-2}$  increases the  $S_{\text{eff}}$  for moderately doped  $n$ -type  $c$ -Si. For higher negative  $Q_f$  values, the  $S_{\text{eff}}$  decreases for  $n$ -type  $c$ -Si, and for a negative  $Q_f > 3 \times 10^{11} \text{ cm}^{-2}$  the  $S_{\text{eff}}$  is practically equal for  $n$ - and  $p$ -type  $c$ -Si. As already mentioned, the surface recombination rate is proportional to the minority carrier concentration at the surface. For a negative  $Q_f$  in the range of  $5 \times 10^{10} - 1 \times 10^{13} \text{ cm}^{-2}$ , electrons are the minority carriers at the surface of both  $n$ - and  $p$ -type  $c$ -Si. The increasing  $S_{\text{eff}}$  for  $n$ -type  $c$ -Si up to a negative  $Q_f$  of  $5 \times 10^{10} \text{ cm}^{-2}$  can be explained by the fact that for this low negative  $Q_f$  holes are still the minority carrier at the  $n$ -type  $c$ -Si surface and the hole concentration, hence the recombination, is increased by electrostatic interaction by the presence of the negative charge at the surface. A similar effect can be observed for  $p$ -type  $c$ -Si passivated by positive charge dielectrics as was shown by Aberle *et al.*<sup>29</sup> For negative  $Q_f > 5 \times 10^{11} \text{ cm}^{-2}$ ,  $S_{\text{eff}}$  scales with  $1/Q_f^2$  for both  $n$ - and  $p$ -type  $c$ -Si. This is in good agreement with the results reported by Kuhlmann *et al.* for inverted  $p$ -type  $c$ -Si surfaces.<sup>37</sup>

The  $Q_f^2$  dependence of the field-effect passivation allows us to compare the relative strength of field-effect passivation by  $\text{Al}_2\text{O}_3$  and other charge containing dielectrics used for  $c$ -Si surface passivation. For thermal  $\text{SiO}_2$  and  $a$ - $\text{SiC}_x$ :H, a relatively low positive  $Q_f$  around  $10^{11} \text{ cm}^{-2}$  on  $p$ -type  $c$ -Si is commonly reported,<sup>29,31,34</sup> whereas for  $a$ - $\text{SiN}_x$ :H, a positive  $Q_f$  in the range of  $10^{12} \text{ cm}^{-2}$  is typically found.<sup>38–40</sup> Consequently, the field-effect passivation provided by  $\text{Al}_2\text{O}_3$  is up to four orders of magnitude stronger compared to thermal  $\text{SiO}_2$  and  $a$ - $\text{SiC}_x$ :H and up to two orders of magnitude stronger compared to  $a$ - $\text{SiN}_x$ :H.

Besides field-effect passivation, chemical passivation also reduces the recombination losses at  $c$ -Si surfaces. For example, the state-of-the-art surface passivation by thermal  $\text{SiO}_2$  can mainly be attributed to chemical passivation due to its extremely low interface defect density. A strong field-effect passivation as in the case of  $\text{Al}_2\text{O}_3$ , however, relaxes

the requirements on the interface defect density. Using the  $Q_f^2$  scaling of the field-effect passivation, we can estimate the relative importance of the chemical passivation for  $\text{Al}_2\text{O}_3$  compared to thermal  $\text{SiO}_2$  for lightly doped  $c$ -Si. Assuming similar electron and hole capture cross sections for the dominant defects, the midgap defect density at the  $c$ -Si surface is allowed to be as high as  $10^{13} \text{ eV}^{-1} \text{ cm}^{-2}$  to yield a similar level of surface passivation compared to thermal  $\text{SiO}_2$  with a midgap interface defect density of  $10^9 \text{ eV}^{-1} \text{ cm}^{-2}$ .<sup>6</sup> However, from Fig. 1, it can be concluded that the  $\text{Al}_2\text{O}_3$  film with the interfacial  $\text{SiO}_x$  film also provides a good level of chemical passivation because the effective lifetime is still relative high at  $\sim 100 \mu\text{s}$  when the negative  $Q_f$  in the  $\text{Al}_2\text{O}_3$  film is balanced (for a poorly passivated surface the effective lifetime would only be  $\sim 5 \mu\text{s}$ ). Hence, the interface defect density between the  $\text{Al}_2\text{O}_3/\text{SiO}_x$  film and the  $c$ -Si substrate is expected to be reasonably low. As can be seen in Table I, typically interface defect densities in the range of  $10^{11} \text{ eV}^{-1} \text{ cm}^{-2}$  have been reported for annealed  $\text{Al}_2\text{O}_3$  films on  $c$ -Si, which is up to two orders of magnitude higher compared to thermal  $\text{SiO}_2$ . Similar to thermal  $\text{SiO}_2$ , the lowest interface defect density is obtained by postdeposition annealing treatments, either an anneal in a  $\text{H}_2$  containing atmosphere in the 300–500 °C temperature range or a short high temperature anneal in  $\text{N}_2$  below the crystallization temperature of  $\text{Al}_2\text{O}_3$ . Moreover, the interface defect density of dielectrics on  $c$ -Si has empirically been related to the average bonding concentration at the interface by Lucovsky *et al.*<sup>41</sup> Dielectrics with an average bonding concentration above 3 would exhibit a high interface defect density and vice versa. As the average bonding concentration of  $\text{Al}_2\text{O}_3$  is 3.6, the interface defect density at the  $c$ -Si surface could be significantly lowered by the presence of a thin  $\text{SiO}_2$ -like film between the  $c$ -Si and the  $\text{Al}_2\text{O}_3$  because  $\text{SiO}_2$  has an average bonding density of 2.8.<sup>41</sup>

The interface defect density is also of relevance due to the fact that interface defect states can trap charges and thereby could potentially cancel part of the field-effect passivation provided by the  $Q_f$  in the passivation film. The influence of the charging of interface defect states on the surface passivation of  $a$ -Si:H on  $c$ -Si has been reported by Garin *et al.*<sup>42</sup> and Obilet *et al.*<sup>43</sup> Nevertheless, the effect of trapped charges becomes only of significance when the interface defect density is of the same order as  $Q_f$ . Hence, for  $\text{Al}_2\text{O}_3$  on  $c$ -Si, it is not expected that this effect can be significant because the defect densities are typically at least one order of magnitude lower than the magnitude of the negative  $Q_f$  in the film (see Table I).

As mentioned,  $\text{Al}_2\text{O}_3$  synthesized by plasma-assisted ALD provides no significant level of surface passivation of  $c$ -Si in the as-deposited state, whereas the level of surface passivation is excellent after a 30 min anneal at 425 °C in  $\text{N}_2$ .<sup>9,10</sup> This difference in surface passivation performance of the  $\text{Al}_2\text{O}_3$  can partly be related to changes in the negative fixed charge density  $Q_f$  after annealing. In Fig. 3, the effective lifetime for  $c$ -Si wafers is shown for  $\text{Al}_2\text{O}_3$  films with a thickness between 6 and 32 nm in the as-deposited and annealed state. The films were deposited on both sides of 275  $\mu\text{m}$  1.9  $\Omega \text{ cm}$   $n$ -type  $c$ -Si wafers by plasma-assisted

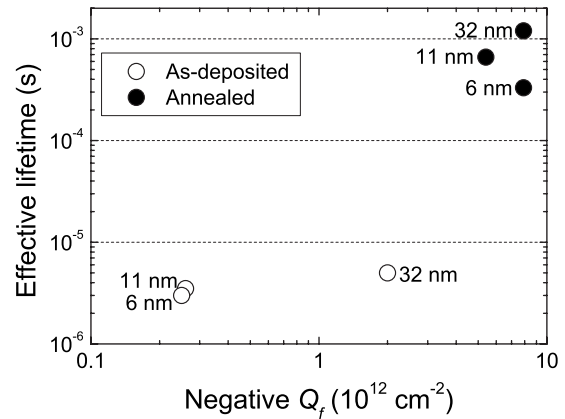


FIG. 3. Measured effective lifetime at an injection level of  $5 \times 10^{14} \text{ cm}^{-3}$  of a 275  $\mu\text{m}$  1.9  $\Omega \text{ cm}$   $n$ -type  $c$ -Si wafer passivated on both sides by a 6, 11, and 32 nm thick  $\text{Al}_2\text{O}_3$  film plotted as a function of the measured negative  $Q_f$  in the  $\text{Al}_2\text{O}_3$  film.  $Q_f$  and the effective lifetime were determined for the as-deposited films and after a subsequent 30 min postdeposition anneal at 425 °C in  $\text{N}_2$ .

ALD at a substrate temperature of 200 °C.<sup>9</sup> The  $Q_f$  in the  $\text{Al}_2\text{O}_3$  films was determined by the contactless optical second-harmonic generation technique (as described in detail in a separate publication<sup>44</sup>), and the effective lifetime was determined by the contactless photoconductance technique. The as-deposited  $\text{Al}_2\text{O}_3$  films already contain a negative  $Q_f$  in the range of  $(3\text{--}20) \times 10^{11} \text{ cm}^{-2}$  without demonstrating any level of surface passivation as indicated by the low effective lifetime in the range of 3–5  $\mu\text{s}$ . After annealing, the negative  $Q_f$  has increased for all films and is within the range of  $(5\text{--}8) \times 10^{12} \text{ cm}^{-2}$ . The effective lifetime also increases over more than two orders of magnitude and reaches a value of 1.2 ms for  $c$ -Si wafer passivated by the 32 nm thick  $\text{Al}_2\text{O}_3$  film. Capacitance-voltage ( $CV$ ) analysis also confirmed the increase in negative  $Q_f$  after the postdeposition anneal.<sup>11</sup> It should also be noted that the negative  $Q_f$  in the as-deposited 32 nm  $\text{Al}_2\text{O}_3$  film of  $2 \times 10^{12} \text{ cm}^{-2}$  is significantly higher compared to the negative  $Q_f$  of  $\sim 3 \times 10^{11} \text{ cm}^{-2}$  that is found in the as-deposited 6 and 11 nm thick  $\text{Al}_2\text{O}_3$  films. This is possibly related to the significant longer deposition time of the 32 nm  $\text{Al}_2\text{O}_3$  film, which leads to an annealing effect during the deposition process itself. The difference in effective lifetime between the annealed 11 and 32 nm  $\text{Al}_2\text{O}_3$  film scales with  $Q_f^2$  and can consequently be attributed to a difference in field-effect passivation. On the other hand, the relative low effective lifetime of the  $c$ -Si wafer passivated by the annealed 6 nm thick film indicates a lower chemical passivation and consequently a higher interface defect density compared to the annealed 11 and 32 nm thick  $\text{Al}_2\text{O}_3$  films.

Using the  $Q_f^2$  scaling of the field-effect passivation, it can be argued that the increase in  $Q_f$  of the 32 nm  $\text{Al}_2\text{O}_3$  film only leads in an increase in the level of field-effect passivation by a factor 16 compared to the  $\text{Al}_2\text{O}_3$  film in the as-deposited state, while the effective lifetime actually increases by more than two orders of magnitude. Consequently the important conclusion can be drawn that the postdeposition anneal also improves the chemical passivation of the 32 nm thick  $\text{Al}_2\text{O}_3$  film by a reduction of the interface defect density. As a matter of fact, the low effective lifetime in combi-

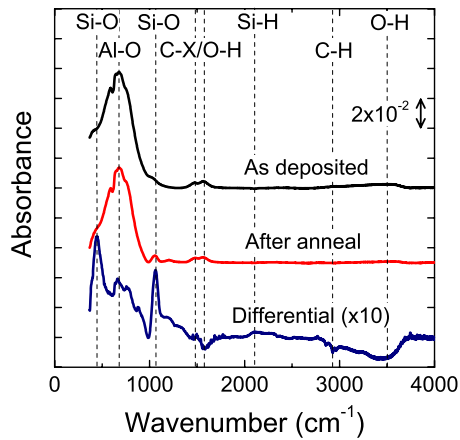


FIG. 4. (Color online) Infrared absorption spectra of a 30 nm thick  $\text{Al}_2\text{O}_3$  film, which was synthesized by plasma-assisted ALD on both sides of a high resistivity  $c$ -Si substrate. Data is presented in the as-deposited and annealed state. Absorption peaks related to Al–O, Si–O, C–H, O–H, and Si–H bonds can clearly be distinguished in the spectra as indicated. For clarity, the differential absorption spectrum is also shown indicating the changes in the  $\text{Al}_2\text{O}_3$  resulting from the postdeposition anneal (positive and negative peaks with respect to the baseline correspond to the appearance and disappearance of absorbing species).

nation with a relative high fixed charge density of  $2 \times 10^{12} \text{ cm}^{-2}$  for the  $c$ -Si wafer passivated by the as-deposited 32 nm  $\text{Al}_2\text{O}_3$  film clearly demonstrates that chemical passivation plays a very important role in the surface passivation mechanism of the annealed  $\text{Al}_2\text{O}_3$  films. The reduction of the interface defect density between the  $\text{Al}_2\text{O}_3$  film and the  $c$ -Si substrate after the postdeposition annealing treatment was also confirmed by  $CV$  measurements, which showed a significant decrease in the parallel conductance.<sup>45</sup> It should be noted that a postdeposition anneal is routinely employed to improve the electrical quality of the interface between  $c$ -Si and dielectric films. This was also demonstrated for the  $c$ -Si/ $\text{Al}_2\text{O}_3$  system in the studies of Hezel and Jaeger<sup>39</sup> and Jeon *et al.*<sup>46</sup> In both studies, the  $c$ -Si/ $\text{Al}_2\text{O}_3$  interface defect density was lowered over more than one order of magnitude (down to  $\sim 1 \times 10^{11} \text{ eV}^{-1} \text{ cm}^{-2}$ ) by a postdeposition annealing step similar to the anneal applied to the  $\text{Al}_2\text{O}_3$  films in Fig. 3.

Other than changes in the bulk and interface electronic properties, structural changes in the  $c$ -Si/ $\text{Al}_2\text{O}_3$  system are also commonly reported after a postdeposition anneal.<sup>20,23</sup> These structural changes are possibly related to the changes in the  $\text{Al}_2\text{O}_3$  bulk and interface electronic properties. HR-TEM revealed the presence of an interfacial oxide layer between the amorphous  $\text{Al}_2\text{O}_3$  film synthesized by plasma-assisted ALD and the  $c$ -Si substrate and this layer slightly increased in thickness from 1.2 nm in the as-deposited state to 1.5 nm after a postdeposition anneal.<sup>9</sup> This interfacial oxide layer consists of  $\text{SiO}_x$  and the presence of Si–O bonds is confirmed by infrared absorbance spectra of as-deposited and annealed  $\text{Al}_2\text{O}_3$  films, as shown in Fig. 4. Particularly after the postdeposition anneal, the Si–O absorption peak in the infrared absorbance spectrum is very similar to the absorption peak observed for good quality thermal  $\text{SiO}_2$ .<sup>47</sup> Chowdhuri *et al.*<sup>20</sup> and Kuse *et al.*<sup>23</sup> also showed a strong increase in Si–O related absorption by infrared spectroscopy and x-ray photoelectron spectroscopy after annealing ALD-

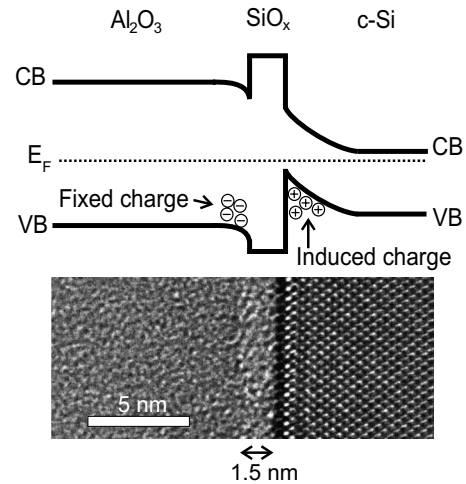


FIG. 5. Schematic band diagram of the  $n$ -type  $c$ -Si/ $\text{SiO}_x/\text{Al}_2\text{O}_3$  system (VB denotes valence band energy, CB denotes conduction band energy, and  $E_F$  denotes Fermi energy). The HR-TEM image shows the  $c$ -Si/ $\text{SiO}_x/\text{Al}_2\text{O}_3$  interface (the black line between the  $\text{SiO}_x$  and  $c$ -Si is a TEM artifact). A high negative  $Q_f$  is present in the  $\text{Al}_2\text{O}_3$  film at the  $\text{Al}_2\text{O}_3/\text{SiO}_x$  interface effectively shields electrons from the  $c$ -Si surface. A relative good interface quality is assured by the presence of a thin interfacial  $\text{SiO}_x$  film between the  $c$ -Si substrate and the  $\text{Al}_2\text{O}_3$  film.

synthesized  $\text{Al}_2\text{O}_3$  films on  $c$ -Si.<sup>20,23</sup> As the absorption intensity of both Si–O and Al–O bonds increase after the postdeposition anneal, it can be argued that the increase in interfacial oxide thickness by TEM can mainly be attributed to a restructuring in the interfacial oxide instead of an additional oxidation of the underlying  $c$ -Si substrate. As mentioned, the interfacial  $\text{SiO}_x$  film could play an important role in the origin of the negative  $Q_f$  in the  $\text{Al}_2\text{O}_3$  film, and hence the changes in the Si–O related absorption could correlate with the change in the magnitude of the negative  $Q_f$  in the  $\text{Al}_2\text{O}_3$  film. The infrared absorbance spectrum in Fig. 4 also confirms the presence of H in the form of O–H groups in the  $\text{Al}_2\text{O}_3$  film. The O–H density decreases after the postdeposition anneal and this decrease coincides with the formation of both Al–O and Si–O bonds. The H atoms released during the anneal can passivate Si dangling bond defects states at the interface as corroborated by an increase in Si–H related absorbance.

## IV. CONCLUSIONS

To summarize, it has been demonstrated that the excellent surface passivation of  $c$ -Si by  $\text{Al}_2\text{O}_3$  films synthesized by plasma-assisted ALD can be explained by a satisfactory low interface defect density in combination with a very high negative  $Q_f$  in the  $\text{Al}_2\text{O}_3$  film. As schematically illustrated in Fig. 5, a high negative  $Q_f$  strongly reduces the electron concentration at the  $c$ -Si interface by means of electrostatic shielding. The negative charges are localized in the  $\text{Al}_2\text{O}_3$  film close to the interface with the  $c$ -Si substrate that is separated from the  $\text{Al}_2\text{O}_3$  through an interfacial  $\text{SiO}_x$  layer. The charges most likely originate from Al vacancies resulting from a preferential tetrahedral coordination of Al in the region close to the interfacial  $\text{SiO}_x$ . The unique negative polarity of  $Q_f$  is especially beneficial for the passivation of  $p$ -type  $c$ -Si, including  $p$ -type emitters on  $n$ -type solar cells, as the bulk minority carriers are shielded from the  $c$ -Si surface.

When the negative  $Q_f$  in the  $\text{Al}_2\text{O}_3$  film is balanced by a positive  $Q_{\text{surface}}$ , still some level of chemical passivation is provided indicating that the interface defect density is also relatively low. The significant improvement in the level of *c*-Si surface passivation by  $\text{Al}_2\text{O}_3$  after a postdeposition anneal can be related to changes in both surface passivating mechanisms, i.e., the negative  $Q_f$  significantly increases and the interface defect density decreases as indicated by the higher quality interfacial  $\text{SiO}_x$ . It has also been addressed that a high negative charge density  $Q_f$  tolerates a relatively high defect density at the *c*-Si interface while maintaining a good level of surface passivation. Because high negative  $Q_f$  values are routinely reported for  $\text{Al}_2\text{O}_3$  films deposited on *c*-Si, irrespective of the deposition technique, it appears that the bulk and interface electrical quality required for excellent surface passivation of *c*-Si are not limited to  $\text{Al}_2\text{O}_3$  films synthesized by ALD but are accessible for a broad range of deposition techniques.

## ACKNOWLEDGMENTS

The authors thank W. Keuning, J. L. van Hemmen, M. J. F. van de Sande, J. F. C. Jansen, and J. J. A. Zeebregts for their technical assistance and their help during the experiments. Dr. I. Martin (Universitat Politecnica de Catalunya) and Dr. J. Schmidt (Institut für Solarenergieforschung Hameln/Emmerthal) are acknowledged for the fruitful discussions on the lifetime data. This work is supported by the Netherlands Technology Foundation STW. The work of B.H. is supported by OTB Solar.

- <sup>1</sup>H. J. Queisser and E. E. Haller, *Science* **281**, 945 (1998).
- <sup>2</sup>M. Boroditsky, I. Gontijo, M. Jackson, R. Vrijen, E. Yablonovitch, T. Krauss, C. C. Cheng, A. Scherer, R. Bhat, and M. Krames, *J. Appl. Phys.* **87**, 3497 (2000).
- <sup>3</sup>M. J. Chen, Y. T. Shih, M. K. Wu, and F. Y. Tsai, *J. Appl. Phys.* **101**, 033130 (2007).
- <sup>4</sup>G. D. Wilk, R. M. Wallace, and J. M. Anthony, *J. Appl. Phys.* **89**, 5243 (2001).
- <sup>5</sup>A. G. Aberle, *Prog. Photovoltaics* **8**, 473 (2000).
- <sup>6</sup>H. Jin, K. J. Weber, N. C. Dang, and W. E. Jellett, *Appl. Phys. Lett.* **90**, 262109 (2007).
- <sup>7</sup>G. Lucovsky, *J. Vac. Sci. Technol. A* **19**, 1553 (2001).
- <sup>8</sup>G. Agostinelli, A. Delabie, P. Vitanov, Z. Alexieva, H. F. W. Dekkers, S. De Wolf, and G. Beaucarne, *Sol. Energy Mater. Sol. Cells* **90**, 3438 (2006).
- <sup>9</sup>B. Hoex, S. B. S. Heil, E. Langereis, M. C. M. van de Sanden, and W. M. M. Kessels, *Appl. Phys. Lett.* **89**, 042112 (2006).
- <sup>10</sup>B. Hoex, J. Schmidt, R. Bock, P. P. Altermatt, M. C. M. van de Sanden, and W. M. M. Kessels, *Appl. Phys. Lett.* **91**, 112107 (2007).
- <sup>11</sup>B. Hoex, J. Schmidt, P. Pohl, M. C. M. van de Sanden, and W. M. M. Kessels, *J. Appl. Phys.* **104**, 044903 (2008).
- <sup>12</sup>J. Schmidt, A. Merkle, R. Brendel, B. Hoex, M. C. M. van de Sanden, and W. M. M. Kessels, *Prog. Photovoltaics* **16**, 461 (2008).
- <sup>13</sup>J. Benick, B. Hoex, M. C. M. van de Sanden, W. M. M. Kessels, O. Schultz, and S. Glunz, *Appl. Phys. Lett.* **92**, 253504 (2008).
- <sup>14</sup>M. Specht, H. Reisinger, F. Hofmann, T. Schulz, E. Landgraf, R. J. Luyken, W. Rosner, M. Grieb, and L. Risch, *Solid-State Electron.* **49**, 716 (2005).
- <sup>15</sup>D. A. Mehta, S. R. Butler, and F. J. Feigl, *J. Appl. Phys.* **43**, 4631 (1972).
- <sup>16</sup>In the studies of Chin *et al.* (Ref. 50) and Duenas *et al.* (Ref. 52) also positive flatband voltage shifts were reported indicating a negative fixed charge density.
- <sup>17</sup>J. A. Aboaf, D. R. Kerr, and E. Bassous, *J. Electrochem. Soc.* **120**, 1103 (1973).
- <sup>18</sup>R. S. Johnson, G. Lucovsky, and I. Baumvol, *J. Vac. Sci. Technol. A* **19**, 1353 (2001).
- <sup>19</sup>S. Y. No, D. Eom, C. S. Hwang, and H. J. Kim, *J. Electrochem. Soc.* **153**, F87 (2006).
- <sup>20</sup>A. Roy Chowdhuri, C. G. Takoudis, R. F. Klie, and N. D. Browning, *Appl. Phys. Lett.* **80**, 4241 (2002).
- <sup>21</sup>S. C. Ha, E. Choi, S. H. Kim, and J. S. Roh, *Thin Solid Films* **476**, 252 (2005).
- <sup>22</sup>R. F. Klie, N. D. Browning, A. R. Chowdhuri, and C. G. Takoudis, *Appl. Phys. Lett.* **83**, 1187 (2003).
- <sup>23</sup>R. Kuse, M. Kundu, T. Yasuda, N. Miyata, and A. Toriumi, *J. Appl. Phys.* **94**, 6411 (2003).
- <sup>24</sup>E. P. Gusev, M. Copel, E. Cartier, I. J. R. Baumvol, C. Krug, and M. A. Gribelyuk, *Appl. Phys. Lett.* **76**, 176 (2000).
- <sup>25</sup>K. Matsunaga, T. Tanaka, T. Yamamoto, and Y. Ikuhara, *Phys. Rev. B* **68**, 085110 (2003).
- <sup>26</sup>P. W. Peacock and J. Robertson, *Appl. Phys. Lett.* **83**, 2025 (2003).
- <sup>27</sup>G. Lucovsky, *J. Vac. Sci. Technol.* **19**, 456 (1981).
- <sup>28</sup>K. Kimoto, Y. Matsui, T. Nabatame, T. Yasuda, T. Mizoguchi, I. Tanaka, and A. Toriumi, *Appl. Phys. Lett.* **83**, 4306 (2003).
- <sup>29</sup>A. G. Aberle, S. Glunz, and W. Warta, *J. Appl. Phys.* **71**, 4422 (1992).
- <sup>30</sup>R. Hezel and R. Schorner, *J. Appl. Phys.* **52**, 3076 (1981).
- <sup>31</sup>I. Martin, M. Vetter, M. Garin, A. Orpella, C. Voz, J. Puigdollers, and R. Alcubilla, *J. Appl. Phys.* **98**, 114912 (2005).
- <sup>32</sup>M. J. Kerr and A. Cuevas, *Semicond. Sci. Technol.* **17**, 166 (2002).
- <sup>33</sup>M. J. Kerr and A. Cuevas, *Semicond. Sci. Technol.* **17**, 35 (2002).
- <sup>34</sup>S. W. Glunz, D. Biro, S. Rein, and W. Warta, *J. Appl. Phys.* **86**, 683 (1999).
- <sup>35</sup>S. Dauwe, L. Mittelstadt, A. Metz, and R. Hezel, *Prog. Photovoltaics* **10**, 271 (2002).
- <sup>36</sup>R. B. M. Girisch, R. P. Mertens, and R. F. Dekeersmaecker, *IEEE Trans. Electron Devices* **35**, 203 (1988).
- <sup>37</sup>B. Kuhlmann, A. G. Aberle, and R. Hezel, Proceedings of the 13th European PVSEC, Nice, France (Stephens Bredford, UK, 1995), p. 1209.
- <sup>38</sup>J. R. Elmiger, R. Schieck, and M. Kunst, *J. Vac. Sci. Technol. A* **15**, 2418 (1997).
- <sup>39</sup>R. Hezel and K. Jaeger, *J. Electrochem. Soc.* **136**, 518 (1989).
- <sup>40</sup>S. Dauwe, J. Schmidt, A. Metz, and R. Hezel, Proceedings of the 29th IEEE Photovoltaic Specialist Conference, New Orleans (IEEE, Piscataway, NJ, 2002), p. 162.
- <sup>41</sup>G. Lucovsky, Y. Wu, H. Niimi, V. Misra, and J. C. Phillips, *Appl. Phys. Lett.* **74**, 2005 (1999).
- <sup>42</sup>M. Garin, U. Rau, W. Brendle, I. Martin, and R. Alcubilla, *J. Appl. Phys.* **98**, 093711 (2005).
- <sup>43</sup>S. Olibet, E. Vallat-Sauvain, and C. Ballif, *Phys. Rev. B* **76**, 035326 (2007).
- <sup>44</sup>J. J. H. Gielis, B. Hoex, M. C. M. van de Sanden, and W. M. M. Kessels, *J. Appl. Phys.* **104**, 073701 (2008).
- <sup>45</sup>E. H. Nicollan and A. Goetzberger, *Bell Syst. Tech. J.* **46**, 1055 (1967).
- <sup>46</sup>I. S. Jeon, J. Park, D. Eom, C. S. Hwang, H. J. Kim, C. J. Park, H. Y. Cho, J. H. Lee, N. I. Lee, and H. K. Kang, *Jpn. J. Appl. Phys., Part 1* **42**, 1222 (2003).
- <sup>47</sup>C. T. Kirk, *Phys. Rev. B* **38**, 1255 (1988).
- <sup>48</sup>G. S. Higashi and C. G. Fleming, *Appl. Phys. Lett.* **55**, 1963 (1989).
- <sup>49</sup>D. G. Park, H. J. Cho, K. Y. Lim, C. Lim, I. S. Yeo, J. S. Roh, and J. W. Park, *J. Appl. Phys.* **89**, 6275 (2001).
- <sup>50</sup>A. Chin, Y. H. Wu, S. B. Chen, C. C. Liao, and W. J. Chen, Proceedings of the VLSI Symposium, Honolulu (IEEE, Piscataway, NJ, 2000), p. 16.
- <sup>51</sup>L. Manchanda, M. D. Morris, M. L. Green, R. B. van Dover, F. Klemens, T. W. Sorsch, P. J. Silverman, G. Wilk, B. Busch, and S. Aravamudan, *Microelectron. Eng.* **59**, 351 (2001).
- <sup>52</sup>S. Duenas, H. Castan, H. Garcia, A. de Castro, L. Bailon, K. Kukli, A. Aidla, J. Aarik, H. Mandar, T. Uustare, J. Lu, and A. Harsta, *J. Appl. Phys.* **99**, 054902 (2006).
- <sup>53</sup>L. Truong, Y. G. Fedorenko, V. V. Afanasev, and A. Stesmans, *Microelectron. Reliab.* **45**, 823 (2005).
- <sup>54</sup>M. Cho, H. B. Park, J. Park, S. W. Lee, C. S. Hwang, J. Jeong, H. S. Kang, and Y. W. Kim, *J. Electrochem. Soc.* **152**, F49 (2005).
- <sup>55</sup>M. Shahjahan, T. Okada, K. Sawada, and M. Ishida, *Jpn. J. Appl. Phys.* **43**, 5404 (2004).
- <sup>56</sup>J. Buckley, B. De Salvo, D. Deleruyelle, M. Gely, G. Nicotra, S. Lombardo, J. F. Damlencourt, P. Hollinger, F. Martin, and S. Deleonibus, *Microelectron. Eng.* **80**, 210 (2005).